Science in China Series E: Technological Sciences

www.scichina.com
tech.scichina.com
www.springerlink.com

Orientation angle workspaces of planar serial three-link manipulators

LI RuiQin[1†], DAI Jian S[2]

[1] College of Mechanical Engineering and Automation, North University of China, Taiyuan 030051, China;
[2] Department of Mechanical Engineering, King's College London, University of London, WC2R 2LS, United Kingdom

This paper presents a classification on the workspaces of planar serial three-link manipulators, that is, position workspace and orientation angle workspace. Position workspace indicates the region reached by the reference point on the end-effector. Orientation angle workspace indicates a set of angle ranges by which the end-effector can reach with certain orientation for every point in the reachable position workspace. By introducing a virtual equivalent mechanism, reachable position workspace can be divided into several Grashof intervals and non-Grashof intervals. The calculation equations of orientation angle workspace are deduced in three situations according to the relationships among four link lengths in the virtual four-bar chain. Three examples are given for three kinds of relationship of link lengths. The orientation angle workspace of extended groups, that is, two of the three link lengths equal, and the orientation angle workspace when the reference point on the end-effector moves along a non-radial direction are also discussed. A program is developed to calculate orientation angle workspaces and output variation curves of orientation angle workspace and key data within the position workspace. The approach and program in this paper can be used for fast calculation and identification of the variation rule of the orientation angle workspace of any given planar serial three-link manipulator on the basis of its link parameters, and for the design of a highly dexterous serial manipulator with proposed link relations.

planar serial manipulator, orientation angle workspace, virtual equivalent mechanism, Grashof criterion

1 Introduction

The workspace is an important performance index of a robot manipulator. The workspace of a planar serial manipulator can be divided into two categories: position workspace and orientation angle workspace. Position workspace indicates the region reached by the reference point on the end-effector. Orientation angle workspace indicates a set of angle ranges by which the end-effector can reach with certain orientation for any point within the reachable position workspace.

Orientation capability characterized by orientation angle workspace is an essential factor associated with robot manipulators. In most applications, robot manipulators are required to reach a set of ranges with certain approaching angles, that is, with a certain orientation. In some cases, full orientation capability, i.e., a 360° full orientation angle workspace is required. Full orientation angle workspace is defined as a space in which a point could be reached from any direction. Partial orientation angle workspace is defined as a space in which a point could be reached from an angle range which is less than 360°. The range magnitude of the orientation angle workspace indicates the dexterous degree of a robot manipulator.

The concept of dexterous workspace was introduced by Kumar et al.[1] in terms of a manipulator hand and classes of manipulator geometries. A composite work

Received July 8, 2008; accepted October 14, 2008
doi: 10.1007/s11431-009-0083-7
†Corresponding author (email: lrq-dyt@nuc.edu.cn)
Supported by the Natural Science Foundation of Shanxi Province (Grant No. 20041070)

space was proposed by Yang et al.[2,3] to represent both position and orientation capabilities of manipulators using Euler parameters, and a dexterous workspace was determined by reducing the composite workspace to the orientation dimension. Dai et al.[4,5] studied mechanism rotatability by introducing a virtual adjustable ground link which connects the end-effector point to the base joint of a planar manipulator to form an equivalent closed-chain mechanism. The approach can identify full orientation capability and partial orientation capability regions. Dai et al.[6,7] developed a finite twist mapping which describes both feasible position and orientation of the end-effector link. In the form of a finite displacement twist, both position and orientation are mapped onto a six-dimensional image space. In particular, in the case of planar manipulators, the finite twist has three elements and is mapped onto a three-dimensional image space with two dimensions representing orientation. The mapping further combines the Cartesian workspace with the configuration space.

In parallel to this part of study, the study on mobility of mechanism linkage attracted much attention. Williams et al.[8,9] developed a new discriminant from an input angle and applied it to mechanism linkage rotatability study. Ting et al.[10] investigated the mobility of planar closed-loop linkages based on the assemblability condition of linkages and the revolvability condition of the input angle in the linkage. Wampler[11] applied polynomial equations to treating mechanism mobility and then used eigenvalue problems to solve for the rotatability of input/output curve. Guo et al.[12] presented a method dividing Grashof region and non-Grashof region of 4*R*1*P*-type five-bar manipulator using characteristics charts and further extended the method to a single loop *N*-bar linkage.

The purpose of this paper is to study the variation rules of orientation angle workspace of planar serial three-link manipulator. Firstly, based on converted equivalent mechanism and further virtual four-bar chain, the regions are divided when the reference point on the end-effector moves along radial direction according to Grashof criterion. The calculation equations of orientation angle workspace are derived for different relationship of link lengths of virtual four-bar chain. Three examples are given for different relationship of serial three link lengths. Then, the orientation angle workspace of extended groups, that is, two of the three link lengths equal, and the orientation angle workspace when reference point on the end-effector moves along non-radial direction are discussed. In the end, a program is developed to output variation curves of orientation angle workspaces only if inputting three link lengths.

2 Rotatability of orientation angle and virtual equivalent principle

Figure 1(a) gives a planar serial three-link manipulator. The lengths of three links are l_1, l_2, l_3, respectively. Link l_3 is the end-effector. Point P is the reference point on the end-effector. The angle γ is the orientation angle. The oscillating range γ_0 of the angle γ for any reference point P within the position workspace is the orientation angle workspace.

By connecting the end-effector point P to the base joint O as a guide way and adding the slider and joint P, the serial three-link manipulator will be converted into a virtual equivalent five-bar linkage with sliding pair. Hence, the study of the orientation of the end-effector is equivalent to the study of the rotatability of the link l_3 in the virtual equivalent five-bar linkage when the end-effector point P moves along radial direction through base joint O, as shown in Figure 1(b).

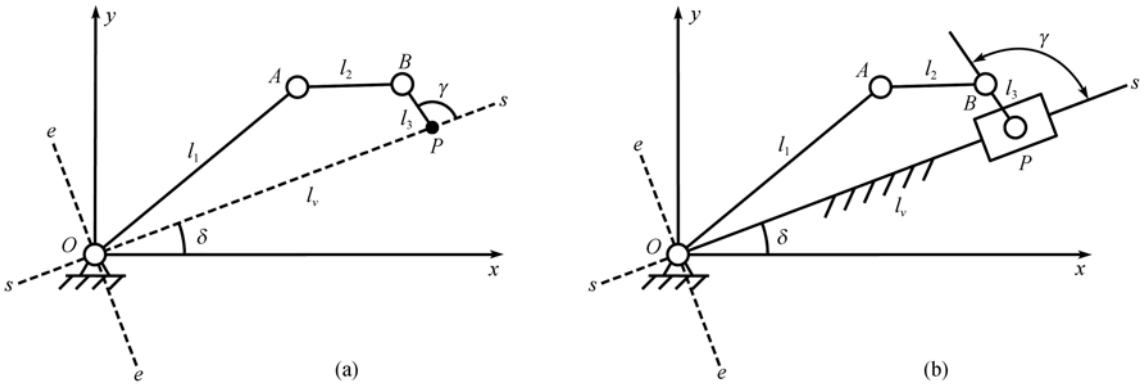

Figure 1 Planar serial manipulator and its virtual equivalent mechanisms.

3 Radial region division based on Grashof criterion

In order to calculate the orientation angle workspace for a definite end-effector point, the virtual equivalent five-bar linkage can be imaged as a four-bar closed chain *OABP* with three links *OA*, *AB*, *BP* of lengths l_1, l_2, l_3 and a virtual link *OP* of variable ground length l_v, as shown in Figure 2. *OP* is called the virtual link l_v. The joint *P* is called the virtual joint *P*. When virtual joint point *P* moves from the furthest point $l_1+l_2+l_3$ towards the center *O* along the coordinate axis *s*-*s* of the reference coordinate system *s*-*e* with any radial direction δ ($\delta\in[0°,360°]$), the length of the virtual link l_v will vary from the longest link, to the intermediate link, and to the shortest link among the four-bars of the virtual four-bar chain *OABP* as follows.

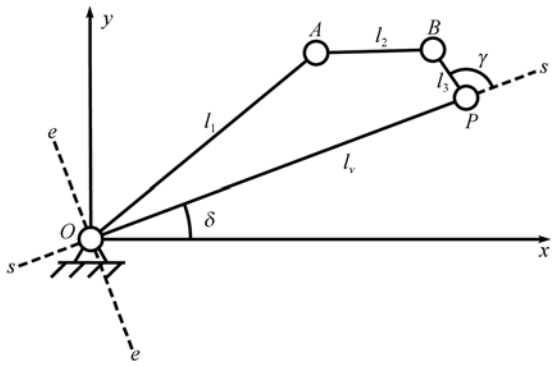

Figure 2 Virtual four-bar chain *OABP*.

1) l_v is the shortest link, if $l_v\leqslant l_{\min}$, where $l_{\min}=\min\{l_i, i=1,2,3\}$.

2) l_v is the intermediate link, if $l_{\min}<l_v<l_{\max}$, where $l_{\max}=\max\{l_i, i=1,2,3\}$.

3) l_v is the longest link, if $l_{\max}\leqslant l_v\leqslant l_{\max}+l_{\mathrm{mid}}+l_{\min}$, where l_{mid} refers to the intermediate link among the three serial links l_1, l_2, l_3.

In order to facilitate dividing the above three regions, a number axis *OS* is setup with its origin placed on the center of the base joint *O* and its direction along *s*-*s* axis from *O* to *P*. On the number axis *OS*, three points are marked as B_1, B_2, B_3 with the coordinate values $S_{B1}=l_{\min}$, $S_{B2}=l_{\max}$, and $S_{B3}=l_{\max}+l_{\mathrm{mid}}+l_{\min}$ as boundary points. The number axis is divided into three sub-regions [0, B_1], [B_1, B_2], [B_2, B_3].

Furthermore, the joint point *P* will impossibly cross the joint point *O* if $l_{\max}>l_{\mathrm{mid}}+l_{\min}$ is satisfied. Hence, the region [0, $l_{\max}-(l_{\mathrm{mid}}+l_{\min})$] on the number axis *OS* cannot be reached by the virtual joint point *P*. The region [0, $l_{\max}-(l_{\mathrm{mid}}+l_{\min})$] is called the inaccessible region. The point with the value $l_{\max}-(l_{\mathrm{mid}}+l_{\min})$ is denoted as A_1 on the number axis *OS*.

As discussed above, the virtual four-bar chain *OABP* will have a variable dimensional relation when the point *P* moves along the number axis *OS*. According to the Grashof criterion, if the sum of the shortest link and the longest link is less than the sum of the remaining two links, the two joints connected to the shortest link are fully revolute joints. Each of the three sub-regions [0, B_1], [B_1, B_2], [B_2, B_3] can be further divided into two parts, the Grashof parts and the non-Grashof parts as follows.

1) In the region [0, B_1], the virtual link l_v is the shortest link. The Grashof condition is $l_v+l_{\max}<l_{\mathrm{mid}}+l_{\min}$. If $l_{\max}<l_{\mathrm{mid}}+l_{\min}$, the region [0, B_1] is divided into Grashof part with $l_v<l_{\mathrm{mid}}+l_{\min}-l_{\max}$ and non-Grashof part with $l_v>l_{\mathrm{mid}}+l_{\min}-l_{\max}$. The point with the coordinate value $l_{\mathrm{mid}}+l_{\min}-l_{\max}$ on the number axis *OS* is denoted as C_1. In the Grashof region [0, C_1], the joint *P* is a full revolute joint and the end-effector link l_3 has a 360° full orientation angle workspace. In the non-Grashof region [C_1, B_1], no joints of full rotatability exist and the end-effector link l_3 has a partial orientation angle workspace, which is less than 360°.

2) In the region [B_1, B_2], the virtual link l_v is the intermediate link. The Grashof condition is $l_{\max}+l_{\min}<l_v+l_{\max}$. The region [$B_1$, B_2] is divided into Grashof part with $l_v>l_{\max}-l_{\mathrm{mid}}+l_{\min}$ and non-Grashof part with $l_v<l_{\max}-l_{\mathrm{mid}}+l_{\min}$. The point with the coordinate value $l_{\max}-l_{\mathrm{mid}}+l_{\min}$ on the number axis *OS* is denoted as C_2. In the Grashof region [C_2, B_2], if the end-effector link l_3 is the shortest link, the end-effector link has a 360° full orientation angle workspace; if the end-effector link l_3 is not the shortest link, the end-effector link l_3 has a partial orientation angle workspace. In the non-Grashof region [B_1, C_2], no joints of full rotatability exist and the end-effector link l_3 has a partial orientation angle workspace.

3) In the region [B_2, B_3], the virtual link l_v is the longest link. The Grashof condition is $l_v+l_{\min}<l_{\max}+l_{\mathrm{mid}}$. The region is divided into Grashof part with $l_v<l_{\max}+l_{\mathrm{mid}}-l_{\min}$ and non-Grashof part with $l_v>l_{\max}+l_{\mathrm{mid}}-l_{\min}$. The point with the coordinate value $l_{\max}+l_{\mathrm{mid}}-l_{\min}$ on the number axis *OS* is denoted as C_3. In the Grashof region

$[B_2, C_3]$, if the end-effector link l_3 is the shortest link, the end-effector link l_3 has a 360° full orientation angle workspace; if the end-effector link l_3 is not the shortest link, the end-effector link l_3 has a partial orientation angle workspace. In the non-Grashof region $[C_3, B_3]$, no joints of full rotatability exist and the end-effector link l_3 has a partial orientation angle workspace.

Therefore, the seven points are denoted on the number axis OS in order to divide Grashof region and non-Grashof region, as shown in Figure 3. The coordinate values of the seven points on the number axis OS are as follows

$$S_{A1} = l_{\max} - (l_{\mathrm{mid}} + l_{\min}), \quad \text{if} \quad l_{\max} > l_{\mathrm{mid}} + l_{\min}, \tag{1}$$

$$S_{B1} = l_{\min}, \tag{2}$$

$$S_{B2} = l_{\max}, \tag{3}$$

$$S_{B3} = l_{\max} + l_{\mathrm{mid}} + l_{\min}, \tag{4}$$

$$S_{C1} = l_{\mathrm{mid}} + l_{\min} - l_{\max}, \quad \text{if} \quad l_{\max} < l_{\mathrm{mid}} + l_{\min}, \tag{5}$$

$$S_{C2} = l_{\max} - l_{\mathrm{mid}} + l_{\min}, \tag{6}$$

$$S_{C3} = l_{\max} + l_{\mathrm{mid}} - l_{\min}. \tag{7}$$

In Figure 3(a), the relation of the serial three link lengths l_1, l_2, l_3 satisfies $l_{\max} < l_{\mathrm{mid}} + l_{\min}$. The moving range of point P is $[0, B_3]$. There are two Grashof regions, $[0, C_1]$ and $[C_2, C_3]$, respectively. The other two regions $[C_1, C_2]$ and $[C_3, B_3]$ are non-Grashof regions.

In Figure 3(b), the relation of the serial three link lengths l_1, l_2, l_3 satisfies $l_{\max} > l_{\mathrm{mid}} + 2l_{\min}$. The coordinate of the point A_1 is located in the region $[B_1, C_2]$. There is only one Grashof region $[C_2, C_3]$. The moving range of the point P is $[A_1, B_3]$.

In Figure 3(c), the relation of the three link lengths l_1, l_2, l_3 satisfies $l_{\mathrm{mid}} + l_{\min} < l_{\max} < l_{\mathrm{mid}} + 2l_{\min}$. The coordinate of point B_1 is larger than the coordinate of point A_1. In the region $[A_1, B_1]$, the virtual link l_v is the shortest link and the relation of the link lengths is $l_v + l_{\max} > l_{\mathrm{mid}} + l_{\min}$. The region $[A_1, B_1]$ is non-Grashof region. There is only one Grashof region $[C_2, C_3]$. The moving range of point P is $[A_1, B_3]$.

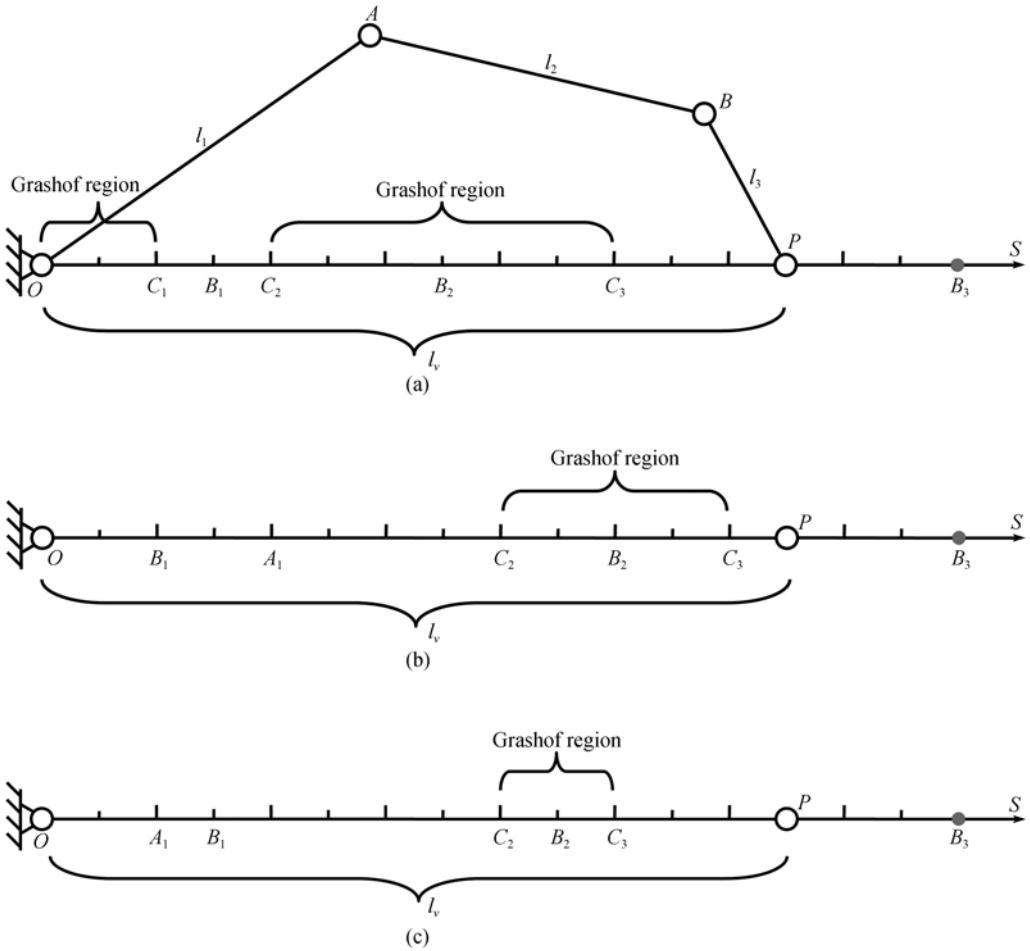

Figure 3 (a) Number axis with $l_{\max} < l_{\mathrm{mid}} + l_{\min}$; (b) number axis with $l_{\max} > l_{\mathrm{mid}} + 2l_{\min}$; (c) number axis with $l_{\mathrm{mid}} + l_{\min} < l_{\max} < l_{\mathrm{mid}} + 2l_{\min}$.

4 Oscillating range of the end-effector link of the virtual four-bar chain

As above discussion, only in the Grashof region and when either the end-effector link or the virtual link is the shortest link, the end-effector link has a full orientation angle workspace. In the other situations, the end-effector link has a partial orientation angle workspace, which is less than 360°. In order to obtain the variation rules of the orientation angle workspace of the end-effector link when the joint point P moves along the number axis OS, it is the key to solve the oscillating range of the end-effector link l_3 around the joint point P according to relations among the link lengths l_1, l_2, l_3, and l_v. The orientation angle workspace is denoted as γ_0.

As shown in Figure 4, in the joint four-bar chain $OABP$, if disconnecting the joint B between link l_2 and link l_3, the locus of the joint point B on the link l_3 is circular with the center P. The moving space of the joint point B on link l_2 is an annulus with radii l_1+l_2 and $|l_1-l_2|$ and with the center O. According to the position relation, the circle with the radius l_3 and the center P and the annulus with the radii l_1+l_2 and $|l_1-l_2|$ and the center O, there exist three situations as follows.

4.1 Situation 1

As shown in Figures 4(a) and (b), if the conditions

$$l_1+l_2 \leqslant l_v+l_3 \quad \text{and} \quad |l_1-l_2| \leqslant |l_v-l_3| \leqslant l_1+l_2, \tag{8}$$

are satisfied simultaneously, the orientation angle workspace γ_0 can be calculated as follows

$$\gamma_0 = \angle B_1PB_2 = 2\arccos\frac{l_v^2+l_3^2-(l_1+l_2)^2}{2l_v\cdot l_3}. \tag{9}$$

4.2 Situation 2

As shown in Figure 4(c), if the conditions

$$l_1+l_2 < l_v+l_3 \quad \text{and} \quad |l_v-l_3| < |l_1-l_2|, \tag{10}$$

are satisfied simultaneously, the orientation angle workspace γ_0 can be calculated as follows

$$\gamma_0 = \angle B_1PB_3 + \angle B_2PB_4$$
$$= 2\arccos\frac{l_v^2+l_3^2-(l_1+l_2)^2}{2l_v\cdot l_3} - 2\arccos\frac{l_v^2+l_3^2-(l_1-l_2)^2}{2l_v\cdot l_3}. \tag{11}$$

4.3 Situation 3

As shown in Figure 4(d), if the conditions

$$|l_v-l_3| \leqslant |l_1-l_2| \quad \text{and} \quad |l_1-l_2| \leqslant l_v+l_3 \leqslant l_1+l_2, \tag{12}$$

are satisfied simultaneously, the orientation angle workspace γ_0 can be calculated as follows

$$\gamma_0 = \angle B_1PB_2 = 360° - 2\arccos\frac{l_v^2+l_3^2-(l_1-l_2)^2}{2l_v\cdot l_3}. \tag{13}$$

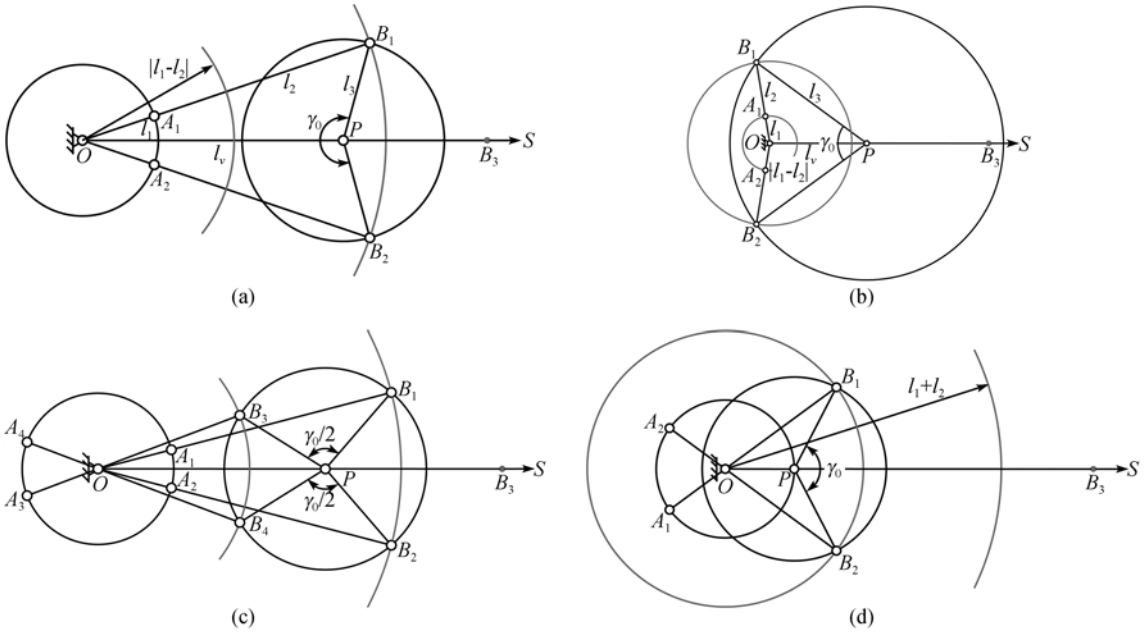

Figure 4 (a) Situation 1 of orientation angle workspace γ_0 with $l_v>l_3$; (b) situation 1 of orientation angle workspace γ_0 with $l_v<l_3$; (c) situation 2 of orientation angle workspace γ_0; (d) situation 3 of orientation angle workspace γ_0.

5 Case studies

A serial three-link manipulator can be categorized into six groups based on the permutation ${}^3P_3=3!=6$. They are shown in Table 1.

Table 1 Groups of the serial three-link manipulators

Group I	Group II	Group III	Group IV	Group V	Group VI
$l_1>l_2>l_3$	$L_2>l_1>l_3$	$l_1>l_3>l_2$	$l_3>l_1>l_2$	$l_2>l_3>l_1$	$l_3>l_2>l_1$

Different groups will obtain different orientation angle workspaces even though using the same three links.

5.1 Example 1: l_{max}=1000, l_{mid}=400, l_{min}=200

The relation among the link lengths satisfies $l_{\max}>l_{\mathrm{mid}}+2l_{\min}$. It belongs to the situation of Figure 3(b). The value of point A_1 is larger than the value of point B_1. Firstly, calculating and marking every interval point on the number axis as shown in Figure 5. Then, solve and compare orientation angle workspaces of Groups I—VI.

$$S_{B1}=l_{\min}=200,\quad S_{A1}=l_{\max}-\left(l_{\mathrm{mid}}+l_{\min}\right)=400,$$

$$S_{C2}=l_{\max}-l_{\mathrm{mid}}+l_{\min}=800,\quad S_{B2}=l_{\max}=1000,$$

$$S_{C3}=l_{\max}+l_{\mathrm{mid}}-l_{\min}=1200,\ S_{B3}=l_{\max}+l_{\mathrm{mid}}+l_{\min}=1600.$$

Group I: $l_1>l_2>l_3$, that is, l_1=1000, l_2=400, l_3=200

The reference point P of the end-effector will move from the furthest distance B_3 to the nearest distance A_1 along the radial direction through the origin of the coordinate O on the number axis OS. With point P moving from the furthest point toward the center O along the radial direction, the reachable range $[A_1, B_3]$ is divided into three regions, two non-Grashof regions $[A_1, C_2]$, $[C_3, B_3]$ and one Grashof region $[C_2, C_3]$.

(i) $l_{v1}\in[C_3, B_3]=[1200, 1600]$

In this region, the virtual link l_{v1} is the longest link. Condition (8) is satisfied, that is,

$$l_{v1}+l_3\geqslant l_1+l_2\ \text{ and }\ \left|l_1-l_2\right|<l_{v1}-l_3\leqslant l_1+l_2.$$

The orientation angle workspace γ_0 can be calculated by using eq. (9) of situation 1 in Figure 4(a).

$$\gamma_0=\angle B_1PB_2=2\arccos\frac{l_{v1}^2+l_3^2-(l_1+l_2)^2}{2l_{v1}\cdot l_3}. \qquad (14)$$

Eq. (14) is the function of the length of the virtual link l_{v1}. With the variation of the length of the virtual link l_{v1} in the interval $[C_3, B_3]$, the variation rule of the orientation angle workspace is depicted as C_3B_3 segment of curve 1 in Figure 6.

(ii) $l_{v2}\in[C_2, C_3]=[800, 1200]$

This is a Grashof region and the shortest link is the end-effector link l_3. Hence, the end-effector link l_3 in this range has a full orientation capacity. This indicates that the end-effector l_3 can reach any position point in this range $[C_2, C_3]$ from any orientation angle.

(iii) $l_{v3}\in[A_1, C_2]=[400, 800]$

In this region, the link l_3 is still the shortest link and the link l_1 is the longest link. Condition (12) is satisfied, that is,

$$\left|l_{v3}-l_3\right|\leqslant\left|l_1-l_2\right|\ \text{ and }\ \left|l_1-l_2\right|\leqslant l_{v3}+l_3<l_1+l_2.$$

The orientation angle workspace γ_0 can be calculated by using eq. (13) of situation 3 in Figure 4(d).

$$\gamma_0=\angle B_1PB_2=360°-2\arccos\frac{l_{v3}^2+l_3^2-\left(l_1-l_2\right)^2}{2l_{v3}\cdot l_3}. \qquad (15)$$

Eq. (15) is the function of the length of the virtual link l_{v3}. With the variation of the length of the virtual link l_{v3} in the interval $[A_1, C_2]$, the variation rule of the orientation angle workspace is depicted as A_1C_2 segment of curve 1 in Figure 6.

Curve 1 in Figure 6 indicates the variation of the orientation angle workspace γ_0 with the virtual link $l_v\in[A_1, B_3]$.

Group II: $l_2>l_1>l_3$, that is, l_1=400, l_2=1000, l_3=200

(i) $l_{v1}\in[C_3, B_3]=[1200, 1600]$

In this region, the virtual link l_{v1} is the longest link. Condition (8) is satisfied, that is,

$$l_{v1}+l_3\geqslant l_1+l_2\ \text{ and }\ \left|l_1-l_2\right|<l_{v1}-l_3\leqslant l_1+l_2.$$

The orientation angle workspace γ_0 can be calculated by using eq. (9) of situation 1 in Figure 4(a).

In fact, from condition (8) and eq. (9), in the situation of exchanging link l_1 and link l_2, the orientation angle workspace does not vary and is the same as Group I in this region.

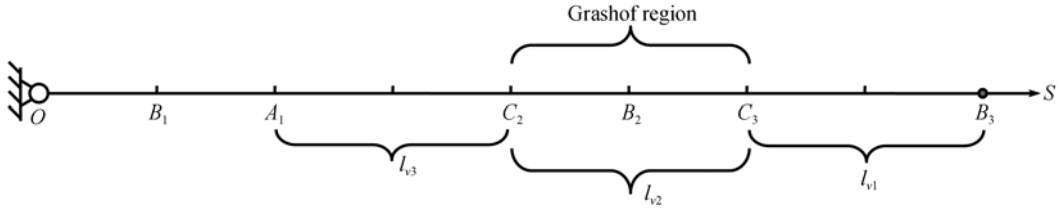

Figure 5 Number axis with $l_{\max}>l_{\mathrm{mid}}+2l_{\min}$.

(ii) $l_{v2} \in [C_2, C_3]=[800, 1200]$

This is a Grashof region and the shortest link is the end-effector link l_3. Hence, the end-effector link l_3 in this range has a full orientation capacity. This indicates that the end-effector l_3 can reach any position point in this range $[C_2, C_3]$ from any orientation angle.

(iii) $l_{v3} \in [A_1, C_2]=[400, 800]$

By comparing with group I, and exchanging link l_1 and link l_2, condition (12) is also satisfied and the orientation angle workspace calculated by using eq. (13) is the same as that in Group I in this region.

The curve of the orientation angle workspace of Group II is the same as curve 1 of Group I.

Group III: $l_1 > l_3 > l_2$, that is, l_1=1000, l_2=200, l_3=400

(i) $l_{v1} \in [C_3, B_3]=[1200, 1600]$

In this region, the virtual link l_{v1} is the longest link. Condition (8) is satisfied, that is,

$$l_1 + l_2 \leqslant l_{v1} + l_3 \quad \text{and} \quad |l_1 - l_2| \leqslant |l_{v1} - l_3| \leqslant l_1 + l_2.$$

The orientation angle workspace γ_0 can be calculated by using eq. (9) of situation 1 in Figure 4(a).

(ii) $l_{v2} \in [C_2, C_3]=[800, 1200]$

Although this is a Grashof region, the shortest link is link l_2. The end-effector link l_3 will oscillate around point P. Condition (10) is satisfied, that is,

$$l_{v2} + l_3 \geqslant l_1 + l_2 \quad \text{and} \quad l_{v2} - l_3 \leqslant l_1 - l_2.$$

The orientation angle workspace γ_0 can be calculated by using eq. (11) of situation 2 in Figure 4(c).

(iii) $l_{v3} \in [A_1, C_2]=[400, 800]$

In this region, condition (12) is satisfied, that is,

$$|l_{v3} - l_3| < |l_1 - l_2| \quad \text{and} \quad |l_1 - l_2| \leqslant l_{v3} + l_3 \leqslant l_1 + l_2.$$

The orientation angle workspace γ_0 can be calculated by using eq. (13) of situation 3 in Figure 4(d).

Curve 2 in Figure 6 indicates the variation of the orientation angle workspace of Group III.

According to a similar analysis, the variation curve of the orientation angle workspace of Group IV($l_3 > l_1 > l_2$) is curve 3 in Figure 6. The variation curve of the orientation angle workspace of Group V($l_2 > l_3 > l_1$) is the same as curve 2 of Group III in Figure 6. The variation curve of the orientation angle workspace of Group VI($l_3 > l_2 > l_1$) is the same as curve 3 of Group IV in Figure 6.

Therefore, we can conclude that the length of the end-effector link is closely related to the curve shape of the orientation angle workspace. When the three links have definite lengths, l_{max}=1000, l_{mid}=400, l_{min}=200, there exist the following relations.

(I) If the end-effector link is the shortest link, we can obtain a largest orientation angle workspace, as shown curve 1 in Figure 6. It has a 360° full orientation angle section, which is corresponding to the length range of the virtual link l_v [800, 1200].

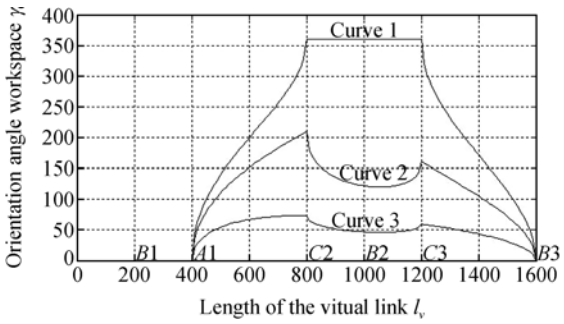

Figure 6 Orientation angle workspaces of Example 1.

(II) If the end-effector link is the longest link, we can obtain a smallest orientation angle workspace, as shown curve 3 in Figure 6. They are all partial orientation angle workspaces for every length of the virtual link l_v.

(III) If the end-effector is the intermediate link, we can obtain an orientation angle workspace whose magnitude is between the largest and smallest orientation angle workspaces, as shown curve 2 in Figure 6.

(IV) When the relation among the link lengths has $l_{max} > l_{mid} + 2l_{min}$, there exists a unreachable region (0, $l_{max} - (l_{mid} + l_{min})$) of the end-effector. In the example, the unreachable region is (0, 400).

5.2 Example 2: l_{max}=700, l_{mid}=600, l_{min}=300

The relation among three link lengths satisfies $l_{max} < l_{mid} + l_{min}$. There is no inaccessible region along any radial direction. Firstly, calculate and mark every interval point on the number axis as shown in Figure 7. Then, solve and compare orientation angle workspaces of Groups I—VI.

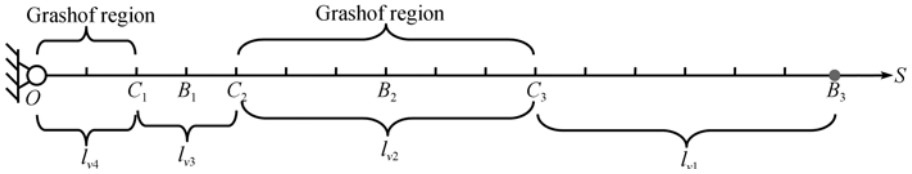

Figure 7 Number axis with $l_{max} < l_{mid} + l_{min}$.

$$S_{C1} = l_{\text{mid}} + l_{\text{min}} - l_{\text{max}} = 200, \quad S_{B1} = l_{\text{min}} = 300,$$
$$S_{C2} = l_{\text{max}} - l_{\text{mid}} + l_{\text{min}} = 400, \quad S_{B2} = l_{\text{max}} = 700,$$
$$S_{C3} = l_{\text{max}} + l_{\text{mid}} - l_{\text{min}} = 1000, \quad S_{B3} = l_{\text{max}} + l_{\text{mid}} + l_{\text{min}} = 1600.$$

According to the procedure of Example 1, the variation curves of orientation angle workspaces of Example 2 can be drawn as shown in Figure 8.

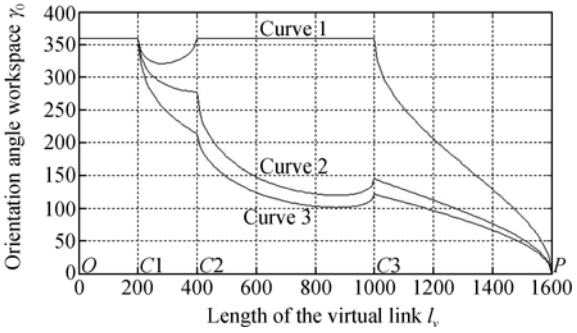

Figure 8 Orientation angle workspaces of Example 2.

Therefore, we can conclude that the length of the end-effector link is closely related to the curve shape of the orientation angle workspace. When the three links have definite lengths, for example, l_{min}=300, l_{mid}=600, l_{max}=700, there exist the following relations.

(I) If the end-effector link is the shortest link, we can obtain a largest orientation angle workspace, as shown curve 1 in Figure 8. It has a 360° full orientation angle section, which is corresponding to the length range of the virtual link l_v [0, 200] and [400, 1000]. In the interval [200, 400], it has also a large orientation angle workspace [321.074, 360].

(II) If the end-effector link is the longest link, we can obtain a smallest orientation angle workspace, as shown curve 3 in Figure 8. It has also a 360° full orientation angle workspace at the interval [0, 200]. Curve 3 is composed of four sections. l_v=400 and l_v=1000 are the two inflection points.

(III) If the end-effector is the intermediate link, we can obtain an orientation angle workspace whose magnitude is between the largest and smallest orientation angle workspaces obtained in the above (I) and (II), as shown curve 2 in Figure 8. Curve 2 is also composed of four sections. l_v=400 and l_v=1000 are also corresponding to the two inflection points.

5.3 Example 3: l_1=900 mm, l_2=400 mm, l_3=300 mm

The relation of the link lengths satisfies $l_{\text{mid}} + l_{\text{min}} < l_{\text{max}} < l_{\text{mid}} + 2l_{\text{min}}$. Hence, there exists a inaccessible region (0, $l_{\text{max}} - (l_{\text{mid}} + l_{\text{min}})$) on the number axis *OS*, as shown in Figure 9. The value S_{A1} of point A_1 is smaller than the value S_{B1} of point B_1.

$$S_{A1} = l_{\text{max}} - (l_{\text{mid}} + l_{\text{min}}) = 200, \quad S_{B1} = l_{\text{min}} = 300,$$
$$S_{C2} = l_{\text{max}} - l_{\text{mid}} + l_{\text{min}} = 800, \quad S_{B2} = l_{\text{max}} = 900,$$
$$S_{C3} = l_{\text{max}} + l_{\text{mid}} - l_{\text{min}} = 1000, \quad S_{B3} = l_{\text{max}} + l_{\text{mid}} + l_{\text{min}} = 1600.$$

As shown in Figure 10, curve 1 indicates the variation of the orientation angle workspace of Group I $l_1 > l_2 > l_3$ and Group II $l_2 > l_1 > l_3$. Curve 2 indicates the variations of the orientation angle workspaces of Group III $l_1 > l_3 > l_2$ and Group V $l_2 > l_3 > l_1$. Curve 3 indicates the variations of the orientation angle workspaces of Group IV $l_3 > l_1 > l_2$ and Group VI $l_3 > l_2 > l_1$.

From the above three examples, the following conclusions can be drawn as follows.

(I) There are three relations of link lengths, $l_{\text{max}} > l_{\text{mid}} + 2l_{\text{min}}$, $l_{\text{max}} < l_{\text{mid}} + l_{\text{min}}$, and $l_{\text{mid}} + l_{\text{min}} < l_{\text{max}} < l_{\text{mid}} + 2l_{\text{min}}$. Under the situation of the same outermost reachable point, the second relation $l_{\text{max}} < l_{\text{mid}} + l_{\text{min}}$ and configurations of Group I $l_1 > l_2 > l_3$ and Group II $l_2 > l_1 > l_3$, the end-effector link is the shortest link. We can obtain the largest orientation angle workspace. As depicted by curve 1 of Groups I and II of Example 2 in Figure 8, there are two sections of full orientation angle workspaces, when the virtual link l_v is in the intervals [0, 200] and [400, 1000].

(II) For any kind of the three relations of link lengths, the orientation angle workspaces of Group I and Group II are the same and are the largest as shown in curve 1 of Figures 6, 8 and 10; the orientation angle workspaces of Groups III and V are the same and less than those of Groups I and II as shown in curve 2 of Figures 6, 8 and 10. The orientation angle workspaces of Groups IV and VI are the same and are the smallest as shown in curve 3 of Figures 6, 8 and 10.

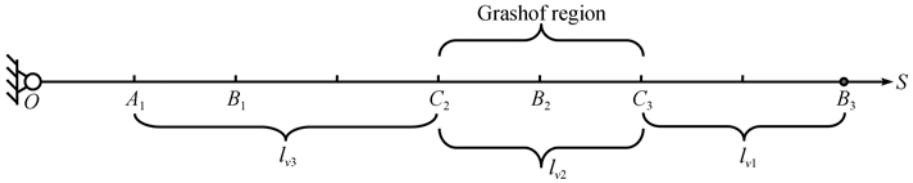

Figure 9 Number axis with $l_{\text{mid}} + l_{\text{min}} < l_{\text{max}} < l_{\text{mid}} + 2l_{\text{min}}$.

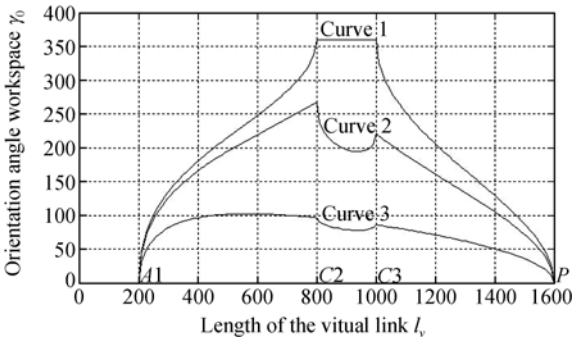

Figure 10 Orientation angle workspaces of Example 3.

6 Non-radial orientation angle workspace of planar serial three-link manipulator

As shown in Figure 11, if the end-effector point P moves along a non-radial guide way $s's'$, $OABP$ is still an equivalent four-bar chain. OP is still virtual ground link l_v. Firstly, according to the previous analysis, every boundary point is calculated. When the link l_1 rotates 360°, the loci of all boundary points are circles.

If $l_{\max} > l_{\text{mid}} + l_{\min}$, in the radial direction Oe', the interval division is the same as the previous discussion. The interval points are A_1, C_2, B_2, C_3, and B_3. In the non-radial direction $s's'$, number axis is $O's'$, the interval points are A_1', C_2', B_2', C_3', and B_3'. The coordinate values can be calculated as follows

$$S_{A1'} = \sqrt{S_{A1}^2 - e^2}, \quad S_{C2'} = \sqrt{S_{C2}^2 - e^2},$$

$$S_{B2'} = \sqrt{S_{B2}^2 - e^2}, \quad S_{C3'} = \sqrt{S_{C3}^2 - e^2}, \; S_{B3'} = \sqrt{S_{B3}^2 - e^2}.$$

The division of non-radial regions is related to the offset e and relation of link lengths. For instance, if $e > C_3$, there is only one non-Grashof region $[O', B_3]$.

In the non-radial number axis $O's'$, the virtual ground link l_v of the virtual four-bar chain can be calculated as follows

$$l_v = \sqrt{l_v'^2 + e^2},$$

where l_v' is the coordinate value on the non-radial number axis $O's'$.

In the non-radial intervals, the calculation of the orientation angle workspace is the same as the previous discussion.

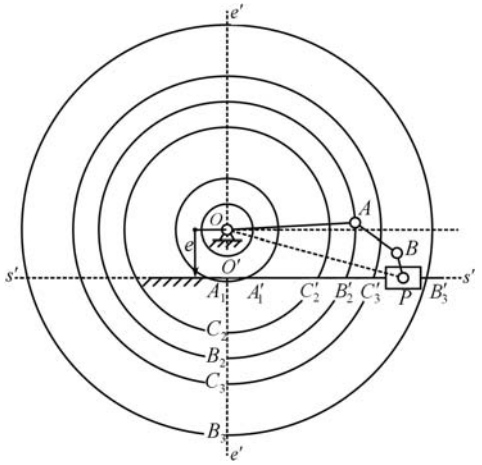

Figure 11 Non-radial interval division .

7 Extended groups of planar serial three-link manipulator

The above Groups I—VI can be extended to the groups where two link lengths are equal. Hence, six extended groups can be given in Table 2.

Table 2 Groups I_{eq}—VI_{eq} with two link lengths equaling

Group I_{eq}	Group II_{eq}	Group III_{eq}	Group IV_{eq}	Group V_{eq}	Group VI_{eq}
$l_1=l_2>l_3$	$l_1=l_3>l_2$	$l_2=l_3>l_1$	$l_1>l_2=l_3$	$l_3>l_1=l_2$	$l_2>l_1=l_3$

Similarly, seven boundary points A_1, C_1, C_2, C_3, B_1, B_2, and B_3 can be calculated according to the previous eqs. (1)—(7). For Groups I_{eq}, II_{eq}, and III_{eq}, the relationship of link lengths is $l_{\max} = l_{\text{mid}} > l_{\min} \rightarrow l_{\max} < l_{\text{mid}} + l_{\min}$, $S_{C1} = S_{B1} = S_{C2} = l_{\min}$, C_1 and C_2 overlap and the corresponding region $[C_1, C_2]$ vanishes. For Groups IV_{eq}, V_{eq}, and VI_{eq}, the relationship of link lengths is $l_{\max} > l_{\text{mid}} = l_{\min}$, $S_{C2} = S_{B2} = S_{C3} = l_{\max}$, the C_2 and C_3 overlap and the corresponding region $[C_2, C_3]$ vanishes. Table 3 illustrates the relationship between the extended Groups I_{eq}—VI_{eq} and the orientation capabilities of the end-effector link.

Table 3 Relationship between extended Groups I_{eq}—VI_{eq} and orientation capabilities

Extended Groups	Relation of link lengths and intervals		Orientation capability	
I_{eq}, II_{eq}, III_{eq}	$l_{\max}=l_{\text{mid}}>l_{\min}$			
I_{eq}, II_{eq}, III_{eq}	$[C_3, B_3]$		Partial	
I_{eq}, II_{eq}, III_{eq}	$[0, C_1]$		Full	
I_{eq}	$[C_2, C_3]$		Full	
II_{eq}, III_{eq}	$[C_2, C_3]$		Partial	
	$l_{\max}>l_{\text{mid}}=l_{\min}$			
IV_{eq}, V_{eq}, VI_{eq}	$l_{\max}<l_{\text{mid}}+l_{\min}$	$l_{\max}>l_{\text{mid}}+l_{\min}$	$l_{\max}<l_{\text{mid}}+l_{\min}$	$l_{\max}>l_{\text{mid}}+l_{\min}$
	$[C_1, B_3]$	$[A_1, B_3]$	Partial	Partial
	$[0, C_1]$		Full	

8 Program flow chart of orientation angle workspace of planar serial three-link manipulator

According to the above analysis, a program has been developed for calculating the orientation angle workspace of planar three-link manipulator. Only inputting the lengths of the three links, l_1, l_2, l_3, can the corresponding curves and key data of the orientation angle workspaces be outputted. The program flow chart is shown in Figure 12.

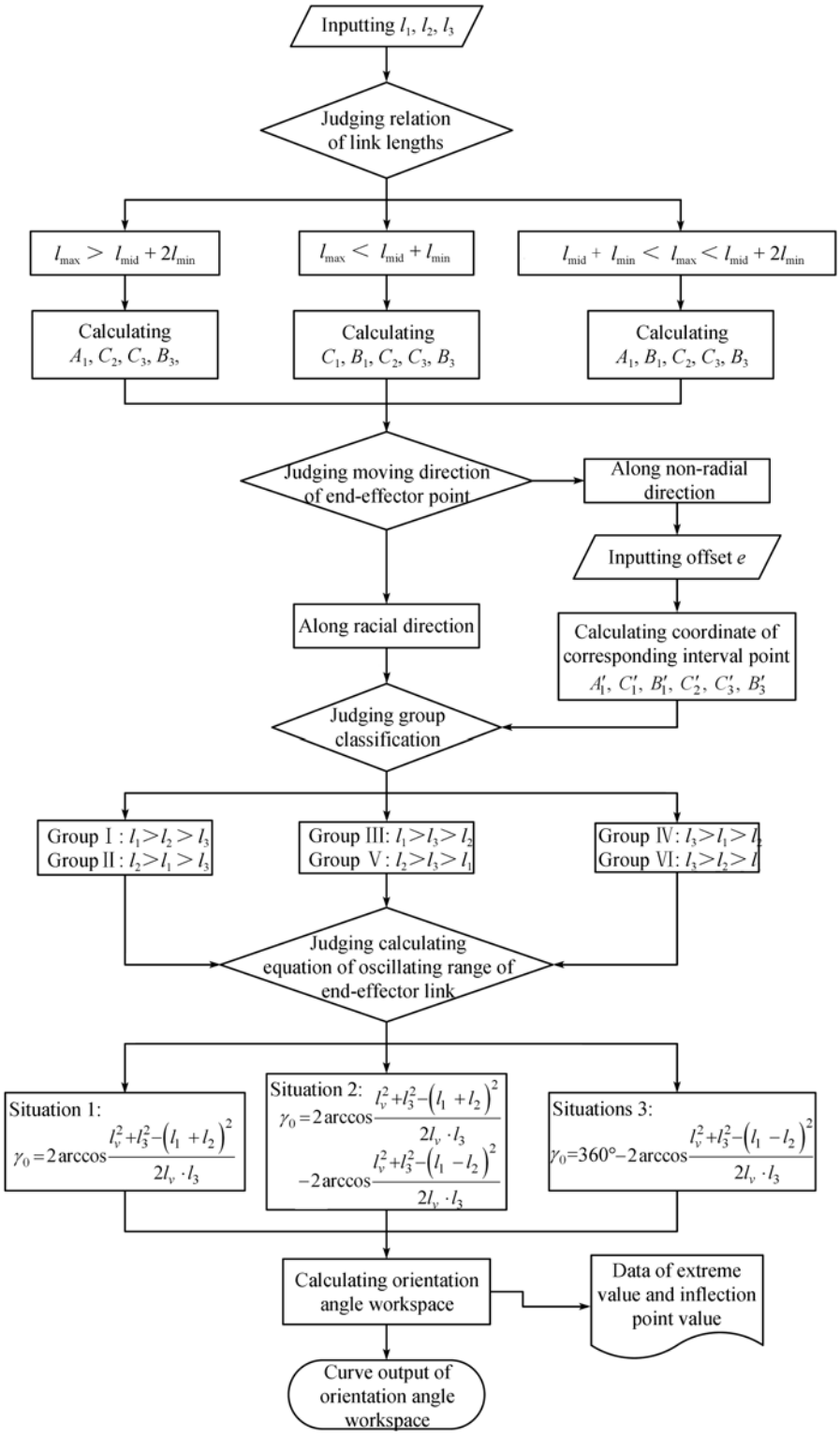

Figure 12 Program flow chart.

9 Conclusions

The orientation angle workspace is an important performance index of a robot manipulator, which indicates the flexible degree of the robot manipulator. By introducing a virtual equivalent mechanism, reachable workspaces can be divided into several intervals according to Grashof criterion. The calculation equations of orientation angle workspace are derived into three situations according to the relationships among the four link lengths in the virtual four-bar chain.

From three examples of three kinds of relationship of link lengths, orientation angle workspaces of Groups I and II are equal and are greater than those of Groups III and V. Orientation angle workspaces of Groups III and V are equal and are greater than those of Groups IV and VI, which are equal. For extended Groups I_{eq}, II_{eq}, and III_{eq}, C_1 and C_2 overlap and the corresponding region $[C_1, C_2]$ vanishes. For extended Groups IV_{eq}, V_{eq}, and VI_{eq}, C_2 and C_3 overlap and the corresponding region $[C_2, C_3]$ vanishes. When the reference point on the end-effector moves along a non-radial direction, the coordinate calculation of region division needs to consider the non-radial offset distance.

The developed program can calculate orientation angle workspaces and output variation curves of orientation angle workspaces and key data. The approach and program in this paper can be used for fast calculation and identification of the variation rule of the orientation angle workspace of any given planar serial three-link manipulator on the basis of its link parameters, and for the design of a highly dexterous serial manipulator with proposed link relations.

1 Kumar A, Waldron K J. The dexterous workspace. ASME Paper No. 80-DET-108, 1980

2 Yang F C, Haug E J. Numerical analysis of the kinematic working capability of mechanisms. ASME J Mech Des, 1994, 116(1): 111－118

3 Yang F C, Haug E J. Numerical analysis of the kinematic dexterity of mechanisms. ASME J Mech Des, 1994, 116(1): 119－126

4 Dai J S, Shah P. Orientation capability of planar serial manipulators using rotatability analysis based on workspace decomposition. Proc Instn Mech Engrs, Part C, J Mech Eng Sci, 2002, 216(C4): 275－288

5 Dai J S, Shah P. Orientation capability of planar manipulators using virtual joint angle analysis. Mech Mach Theory, 2003, 38(3): 241－252

6 Dai J S, Holland N, Kerr D R. Finite twist mapping and its application to planar serial manipulators with revolute joints. Proc Instn Mech Engrs, Part C, J Mech Eng Sci, 1995, 209(C3): 263－271

7 Dai J S, Kerr D R. Analysis and synthesis of planar grasping in an image space. In: Proceedings of 22nd ASME Biennial Mechanisms Conference, Scottsdale, Arizona, September 1992, DE-45: 283－292

8 Williams R L, Reinholtz C F. Proof of Grashof's law using polynomial discriminants. ASME J Mech, Transm, Autom Des,1986, 108(4): 562－564

9 Williams R L, Reinholtz C F. Mechanism link rotatability and limit position analysis using polynomial discriminants. ASME J Mech, Transm, Autom Des, 1987, 109(2): 178－182

10 Ting K L, Liu Y W. Rotatability laws for *N*-bar kinematic chains and their proofs. ASME J Mech Des, 1991, 113(3): 32－39

11 Wampler C W. Solving the kinematics of planar mechanisms. ASME J Mech Des, 1999, 121(3): 387－391

12 Guo W Z, DU R, Wang J X. On the mobility of single loop *N*-bar linkage with one prismatic joint. In: ASME Design Engineering Technical Conferences and Computers and Information in Engineering Conference, Long Beach, California, USA, 2005